Infection and Drug Resistance

Dovepress
open access to scientific and medical research

Open Access Full Text Article

ORIGINAL RESEARCH

Retrospective Analysis of 10 Cases of Disseminated Nontuberculous Mycobacterial Disease with Osteolytic Lesions

Mengxin Tang,[1,2,*] Jie Huang,[3,*] Wen Zeng,[1,2] Yanmei Huang,[4] Yaoqiang Lei,[5] Ye Qiu,[6] Jianquan Zhang[1,2,4]

[1]Department of Respiratory and Critical Medicine, The First Affiliated Hospital of Guangxi Medical University, Nanning, Guangxi, 530021, People's Republic of China; [2]Guangxi Medical University, Nanning, Guangxi, 530021, People's Republic of China; [3]Department of Tuberculosis Ward, Nanning Fourth People's Hospital, Nanning, Guangxi, 530021, People's Republic of China; [4]Department of Respiratory and Critical Medicine, The Eighth Affiliated Hospital, Sun Yat-sen University, Shenzhen, Guangdong, 518000, People's Republic of China; [5]Department of Infectious Diseases, Yongning District People's Hospital, Nanning, Guangxi, 530021, People's Republic of China; [6]Department of Comprehensive Internal Medicine, The Affiliated Tumor Hospital of Guangxi Medical University, Nanning, Guangxi, 530021, People's Republic of China

*These authors contributed equally to this work

Correspondence: Ye Qiu
Department of Comprehensive Internal Medicine, The Affiliated Tumor Hospital of Guangxi Medical University, Nanning, Guangxi, 530021, People's Republic of China
Tel +8615676192180
Fax +86771–5719573
Email yeqiu2013graduated@163.com

Jianquan Zhang
Department of Respiratory and Critical Medicine, The First Affiliated Hospital of Guangxi Medical University, Nanning, Guangxi, 530021, People's Republic of China
Tel +8613978123845
Fax +86755-23482484
Email jqzhang2002@126.com

Purpose: Disseminated nontuberculous mycobacterial (DNTM) infection can involve multiple organs, including the lungs, skin and soft tissues and lymph nodes. However, NTM infection leading to osteolysis has been rarely reported. Here, we analyzed the clinical features, osteolytic mechanisms, treatment and prognosis of patients with DNTM disease with osteolytic lesions.

Patients and Methods: This retrospective study was conducted between January 1, 2011, and December 31, 2020, at the First Affiliated Hospital of Guangxi Medical University and the Fourth People's Hospital of Nanning City. Patients who had culture and/or histopathological proof of DNTM disease with osteolytic lesions were included.

Results: Ten HIV-negative patients with DNTM disease with osteolytic lesions were enrolled. Five of these patients had underlying diseases. Seven and three of the patients were positive and negative for anti-interferon-γ autoantibodies (AIGAs), respectively. The AIGA positivity rate was 70% (7/10). Ostealgia and anemia were the most common symptoms, followed by fever, emaciation, cough, expectoration, anorexia, subcutaneous abscesses and lymphadenopathy. Leukocyte and neutrophil counts were increased. The most common sites were the vertebrae, sternum, clavicle and ribs, although the femur, ilium, humerus, and scapula were also involved. Radiography and computed tomography (CT) showed moth-eaten or irregular destruction of bone, bone defects, pathological fracture, periosteal proliferation and surrounding abscesses. Emission CT (ECT) bone scans showed significantly increased uptake in many skeletal regions. Positron emission tomography(PET)/CT showed metabolic activity in multiple bones. All patients received anti-nontuberculous therapy, and five underwent surgery. Two died during treatment.

Conclusion: DNTM infection of bone and leading to osteolysis usually occurs in patients with AIGA-positive antibodies. DNTM disease with osteolysis is characterized by increased leukocytes and neutrophil counts, focal suppurative granulomas, and multiple areas with moth-eaten or irregular destruction of bone with increased radioactive concentrations. Early diagnosis and timely, effective combination anti-NTM therapy can improve the prognosis.

Keywords: HIV-negative, nontuberculous mycobacteria, osteolytic lesion, anti-IFN-γ autoantibodies

Introduction

Nontuberculous mycobacterial (NTM) infection can lead to disseminated NTM (DNTM) disease, which usually affects multiple organs including the lung, skin and soft tissues and lymph nodes, as well as and bone can also be affected.[1,2] Previously, NTM infection of bone leading to osteolysis has been rarely reported

Received: 6 September 2021
Accepted: 26 October 2021
Published: 9 November 2021

and is often overlooked by clinicians. Recent research revealed that 34% of anti-IFN-γ-autoantibody (AIGA)-associated NTM disease can involve the bone and joints,[3] suggesting that NTM infection of bone is not rare in AIGA-positive NTM patients. However, the mechanism of NTM leading to osteolysis is unclear, and it may be related to AIGAs.[4,5] Osteolytic destruction due to NTM is frequently misdiagnosed as tuberculosis or other fungal infections,[6–8] indicating insufficient recognition of this condition by clinicians. Moreover, systemic research on the clinical and imaging characteristics of patients with NTM involving bone and leading to osteolytic lesions is lacking, leading to delays in correct diagnosis and treatment. Therefore, we retrospectively analyzed the clinical and imaging characteristics of 10 human immunodeficiency virus (HIV)-negative patients with DNTM disease with osteolytic lesions to provide clinical experience for the early diagnosis of this condition.

Patients and Methods

Study Population

The medical records of ten HIV-negative patients diagnosed with DNTM disease with osteolytic lesions between January 1, 2011, and December 31, 2020, at the First Affiliated Hospital of Guangxi Medical University and the Fourth People's Hospital of Nanning City were retrospectively evaluated. Data extracted from the medical records included demographic information (sex, age and occupation), clinical characteristics, laboratory findings, imaging manifestations, and clinical outcomes.

This study was approved by the Signation Ethical Committee of the First Affiliated Hospital of Guangxi Medical University [2021[KY-E-118]]. All patients or patients' parents provided written informed consent.

Methods Used to Diagnose NTM Infection

Patients were diagnosed with NTM infection according to the following criteria: 1) NTM culture: Clinical specimens (such as sputum, blood, skin lesion pus, bone marrow, and pathological tissues) were inoculated on solid and liquid medium and incubated at 35°C. Positive RGM cultures were characterized by colonies that were visible to the naked eye within 7 days, while positive SGM cultures by colonies formed within 2 to 3 weeks.[9,10] 2) Identification of NTM species: Gene sequencing technology, such as direct homologous gene method or sequence alignment method (16S DNA, hsp65), is currently the "gold standard" for strain identification.[10,11] Previously, due to the limitation of the laboratory conditions, only species were identified, but no subspecies were identified. Patients who met one of the above criteria were diagnosed with NTM infection.

Diagnostic Criteria for DNTM Disease

The diagnostic criteria for DNTM disease were as follows: two or more nonadjacent tissues or organs were involved, positive NTM culture/positive molecular biology detection from the blood, and/or positive NTM culture/positive molecular biology detection from any of the following: respiratory secretions, skin lesion pus, bone marrow, and biopsy specimens from the liver, lymph nodes, and lung.[9]

Diagnostic Criteria for NTM with Osteolytic Lesions

Patients were diagnosed according to one of the following criteria: 1) NTM identified in bone and/or bone marrow biopsy samples using culture and metagenomics next-generation sequencing (mNGS); 2) disseminated NTM disease with osteolytic lesions diagnosed based on the presence of osteolytic lesions on imaging examination, clinical symptoms including ostealgia, improvement after receiving anti-NTM treatment alone, and exclusion of other diseases that cause osteolysis (tuberculosis, cancer, hematological diseases, and fungal infections such as *African histoplasmosis, blastomycosis, cryptococcosis, Talaromycosis marneffei* and *coccidioidomycosis*).

Anti-IFN-γ Autoantibody Assay

Serum samples were obtained under sterile conditions before the patient received antimicrobial therapy and during the active stage of the infection. Serum samples were retrieved from a serum bank and stored at −80°C. AIGAs antibody was detected in all participants. All serum samples were tested at the first thaw. The detection of AIGAs in the serum was performed using an enzyme-linked immunosorbent assay kit (Cloud-Clone Corp., Wuhan, China) according to the manufacturer's protocols. The normal range for the AIGA concentration was defined as the 99th percentile for the healthy controls and was estimated using the log-normal distribution. Outlying concentrations were classified as positive for AIGAs.[13]

Results

Demographic Data, Clinical Characteristics, NTM Culture and Histopathology

During the 10-year study period, ten HIV-negative patients with DNTM disease with osteolytic lesions were evaluated. The study population included six males with a median age of 54.5 years (range 36.5–74.25 years). Their occupations included farmers (n = 7), retirees (n = 2) and workers (n = 1). The median time from symptom onset to diagnosis was 12 months (range: 8.5–18.5 months). Among the ten patients, five patients had 1–2 underlying diseases and/or a previous surgical history, and two (20%) had previous glucocorticoid therapy. Six patients had other bacterial and fungal coinfections. All patients showed disseminated infection of NTM, with the lung, lymph nodes, skin, bone, joint, and liver being the most commonly involved organs. Microbiological studies demonstrated *M. abscessus* in three patients, *M. avium* complex in two patients, and *M. kansasii, M. fortuitum, M. chelonae, M. intracellulare*, and *M. intermedium* in one patient each. NTM were isolated from sputum samples (6/10, 60%), pus from subcutaneous abscesses (5/10, 50%), pus from joints (1/10, 10%), pus from lymph nodes (1/10, 10%) and bronchoalveolar lavage fluid (1/10, 10%). In addition, histopathology or cytology of specimens obtained from five patients showed suppurative inflammation, including 2 with and 3 without granuloma formation. All patients were misdiagnosed with tuberculosis (including pulmonary tuberculosis, bone and joint tuberculosis, lymph node tuberculosis, and tuberculous pleurisy), and the duration of antituberculosis treatment varied from 4 to 48 months (Table 1).

Anemia (100%) and ostealgia (100%) were the most common symptoms and signs, followed by fever (70%), emaciation (70%), cough and expectoration (70%), subcutaneous abscesses (70%), anorexia (60%) and lymphadenopathy (60%). Joint pain (10%), joint dysfunction (10%), abdominal pain and distension (10%), diarrhea (10%) and bloody stool (10%) were also present (Supplemental Table 1).

Laboratory Examination

Complete blood count examinations revealed increased white blood cell and neutrophil counts in nine patients (90%) (median 14.65 × 10^9/L, range 11.85–22.1× 10^9/L; median 11.49 × 10^9/L, range 8.64–18.7 × 10^9/L, respectively) and normal absolute lymphocyte counts in ten patients. Ten patients showed decreased hemoglobin concentrations (median 83 g/L, range 68.65–96.25 g/L). Four of nine patients showed reductions in CD4+ T lymphocyte counts (median 511 cells/μL, range 182–614 cells/μL). Three of nine patients showed reductions in CD8+ T lymphocyte counts (median 331 cells/μL, range 122.5–429.5 cells/μL). Nine patients (90%) showed decreased albumin levels (median 29.4 g/L, range 24.5–33.6 g/L), four patients (40%) showed decreased globulin levels (median 39.5, range 35.2–46.2 g/L), and three patients (30%) showed liver dysfunction. C-reactive protein (CRP) concentrations and erythrocyte sedimentation rate (ESR) were significantly increased in all patients (median 101 mm/h, range 45.5–133 mm/h; median 134 mg/L, range 69.6–175.6 mg/L, respectively). Serum samples obtained from 10 patients were tested for AIGAs. Among the ten patients, seven patients were defined as AIGA-positive, and the other three were defined as AIGA-negative. The positivity rate of AIGAs was 70% (7/10), with a median titer of 31,220.2 ng/mL and a range of 4266.2–56,088.2 ng/mL (Supplemental Table 2).

Skeletal Localization

NTM could affect any bone of the body, presenting with multiple bone involvement. The bony structures involved were as follows: bones of the limbs (6/9, 66.67%), trunk (5/9, 55.56%), skull 2/9, 22.22%), and cartilage (1/9, 11.11%). The most common sites were the vertebrae, sternum, clavicle, and ribs (3/9, 33.33%). The femur and ilium were affected in two patients (2/9, 22.22%), and the humerus, scapula, metacarpal, phalanx, tibia, talus, frontal bone and mandible were affected in one patient (1/9,11.11%). Two patients (2/9, 22.22%) showed joint involvement, and seven patients showed surrounding abscess formation (7/9, 77.78%) (Table 1).

Image Features of Disseminated NTM Disease with Osteolytic Lesions

All patients showed multiple areas with osteolytic destruction (more than two sites). Radiographic and CT examinations were performed on nine patients and showed moth-eaten or irregular destruction of bone, bone defects, and single/multiple, well-circumscribed, rounded low-density areas with bone destruction (Figure 1). Pathological fracture was identified in two patients (Figure 1A), periosteal proliferation in two patients (Figure 1F), and surrounding abscess formation in seven

Table 1 Demographic Data, Clinical Characteristics, NTM Culture and Histopathology of 10 Patients with Disseminated Nontuberculous Mycobacterial Disease with Osteolytic Lesions

No.	Age/ Sex	Occupation	AIGAs	Medical History	Site(s) of Organ Involvement	Site(s) of Bone Involvement	Site(s) of Positive Culture	Pathogen	Histopathology	Concurrent Infections	Misdiagnosis	Antituberculosis Therapy (M)
P1-SGM	73y/F	Worker	Positive	COPD Rheumatoid disease	Lung, skin, bone	Sternum, ribs	Sputum	*M. kansasii*	Chest wall mass with suppurative inflammation	*Aspergillus, Candida albicans*	TB	18
P2-RGM	80y/M	Farmer	Positive	Left mandibular fracture	Lymph node, bone, bone marrow	Mandible	Pus from left maxillofacial area	*M. abscessus*	None	None	TB	1
P3-RGM	62y/M	Farmer	Negative	Systemic scleroderma	Lung, bone and joints	Bones of the fingers, metacarpus, ilium, femur, wrist joint, hip joint, cartilage	Pus from right wrist joint	*M. fortuitum*	None	None	TB	5
P4-RGM	68y/M	Retiree	Negative	DM hyperthyroidism	Lung, skin, bone	Cervical spine, thoracic spine	Sputum, pus from chest wall and back	*M. chelonae*	None	*Candida albicans*	TB	48
P5-SGM	78y/F	Farmer	Positive	Previously healthy	Lung, skin, bone, lymph node	Frontal bone, clavicle	Sputum, pus from right parotid area	*M. intracellulare*	Mass on right parotid area with suppurative granuloma	*Talaromyces marneffei, Candida albicans, Staphylococcus epidermidis*	TB	19
P6-SGM	39y/F	Retiree	Negative	DM breast cancer	Lung, skin, bone	Sternum, ribs, clavicle, scapula, humerus	Sputum	*M. avium complex*	None	*Enterococcus faecalis, Pseudomonas aeruginosa*	TB	15

P7-SGM	37y/F	Farmer	Positive	Previously healthy	Lung, lymph node, bone, liver, spleen	Tibia, talus	Sputum, BALF	*M. avium complex*	Pulmonary mass with suppurative inflammation; supraclavicular lymph nodes with necrotizing lymphadenitis	None	TB	12
P8-RGM	35y/M	Farmer	Positive	Previously healthy	Lung, lymph node, bone	Sternum, ribs, thoracic spine lumbar spine, sacrum, ilium, femur, knee joint, sacroiliac joint	Pus from cervical lymph node	*M. abscessus*	None	*Talaromyces marneffei*	TB	12
P9-SGM	47y/M	Farmer	Positive	Previously healthy	Bronchi and lung, lymph node, skin, bone	Multiple areas of bone destruction throughout the body	Sputum, pus from left lateral malleolus	*M. intermedium*	Bronchial nodule in the upper lobe of the left lung with chronic suppurative inflammation of bronchial mucosa	*Talaromyces marneffei, Escherichia coli, Staphylococcus hominis, Burkholderia cepacia*	TB	4
P10-RGM	30y/M	Farmer	Negative	Previously healthy	Lymph node, bone, liver	lumbar spine, cervical spine, clavicle	Pus from the right iliac area	*M. abscessus*	Mass on the right iliac area with suppurative granuloma	None	TB	12

Abbreviations: BALF, bronchoalveolar lavage fluid; COPD, chronic obstructive pulmonary disease; DM, diabetes mellitus; RGM, rapidly growing mycobacteria; SGM, slowly growing mycobacteria; TB, tuberculosis.

https://doi.org/10.2147/IDR.S337956

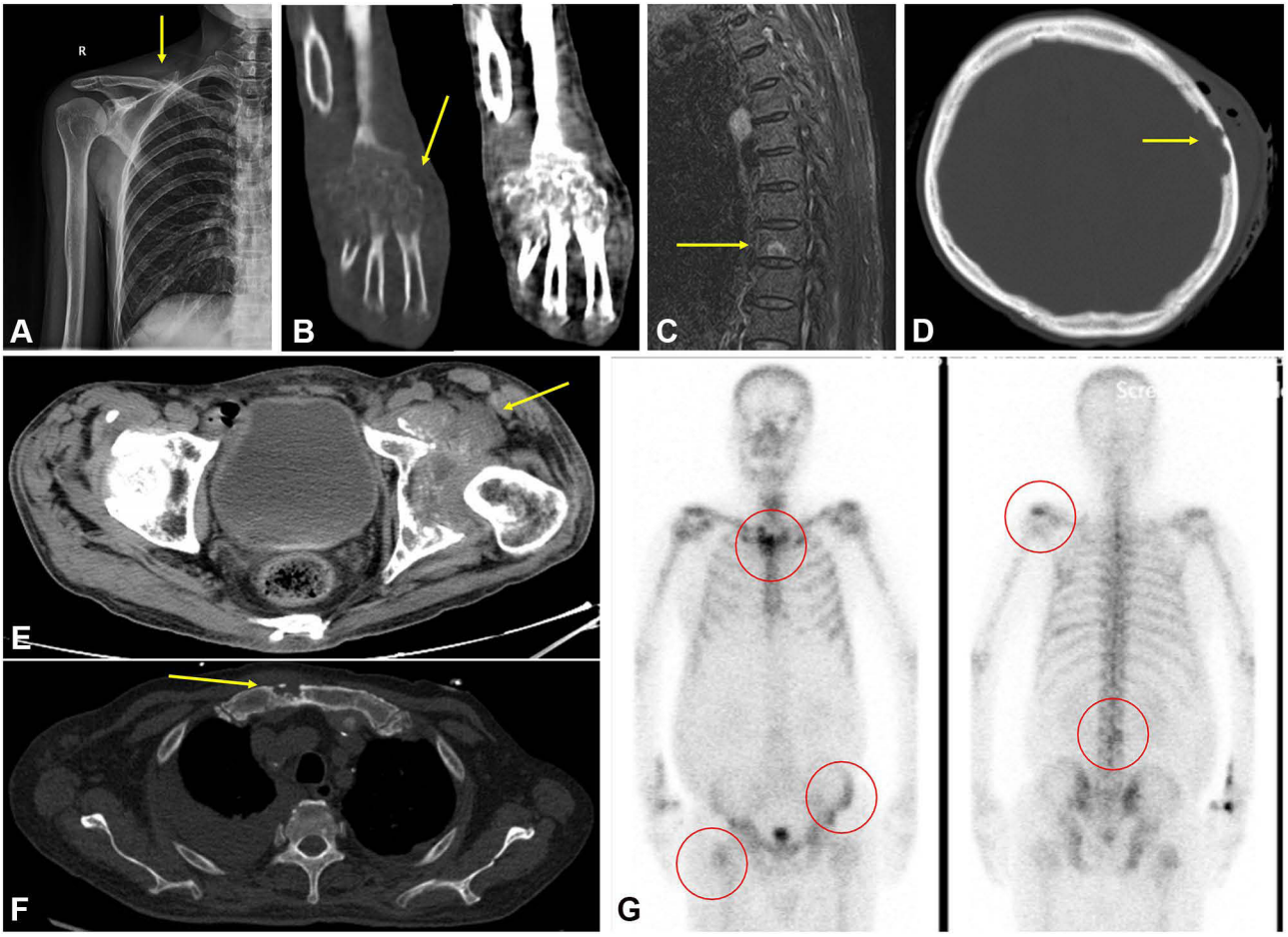

Figure 1 X-ray radiography revealed a pathological fracture in the right clavicle (arrow) (**A** from patient 5). CT of the right wrist and palm revealed moth-eaten and irregular destruction of the bone in the right metacarpal and adjacent joints, narrowing of the joint space and swelling in the surrounding soft tissues (arrow) (**B** from patient 3). A sagittal magnetic resonance imaging (MRI) scan (fat-saturated T2-weighted image) revealed high signals within the L3 vertebral body (arrow) (**C** from patient 8). Computed tomography (CT) of the head and brain revealed irregular destruction of the bone in the inner plate of the left frontal bone with surrounding abscess formation (arrow) (**D** from patient 5). Pelvic CT revealed irregular destruction of the bone in the left acetabulum and femoral head, narrowing of the hip joint space, and surrounding abscess formation (arrow) (**E** from patient 3). Chest CT scan revealed an irregular bone defect in the manubrium of the sternum with a sclerotic edge (arrow) (**F** from patient 8). ECT bone scan revealed increased radioactive concentrations in the manubrium of the sternum, multiple ribs, L3 vertebral body, bilateral sacroiliac joints, left ilium, and upper end of the right femur (**G** from patient 8).

patients (Figure 1B, D and E). A magnetic resonance imaging (MRI) scan was performed on one patient and showed high signals in the T2-weighted image and the fat-saturated T2-weighted image (Figure 1C). An ECT bone scan was performed in one patient and showed significantly increased uptake in multiple bones (Figure 1G). Positron emission tomography/CT (PET/CT) was performed in two patients and showed metabolic activity in multiple bones of the body, indicating systemic bone marrow involvement. Chest computed tomography (CT) revealed abnormal findings in eight patients, presenting as patchy exudation, fiber proliferation, consolidation, bronchiectasis, ground-glass opacity, cavities, atelectasis, nodules, mediastinal and/or hilar lymphadenopathy, pleural thickening, pleural effusion and pericardial effusion (Figure 2 and Table 2).

Treatments and Outcomes

All patients received anti-nontuberculous therapy with a combination of 2–5 types of antibiotics dominated by clarithromycin after antimicrobial susceptibility testing (AST) of NTM Infections. Six patients received sensitive drugs for other bacterial and fungal coinfections. In addition to medical treatment, five patients underwent surgery (50%), consisting of debridement, incision for drainage and internal fixation. Seven patients improved, five of whom were cured after the initial treatment, but the other two were cured after changing the therapeutic regimen many times due to the aggravation of symptoms or recurrence. The duration of treatment ranged from 18 to 65 months. Patient 3, who had joint dysfunction that influenced activities of daily living, recovered completely after

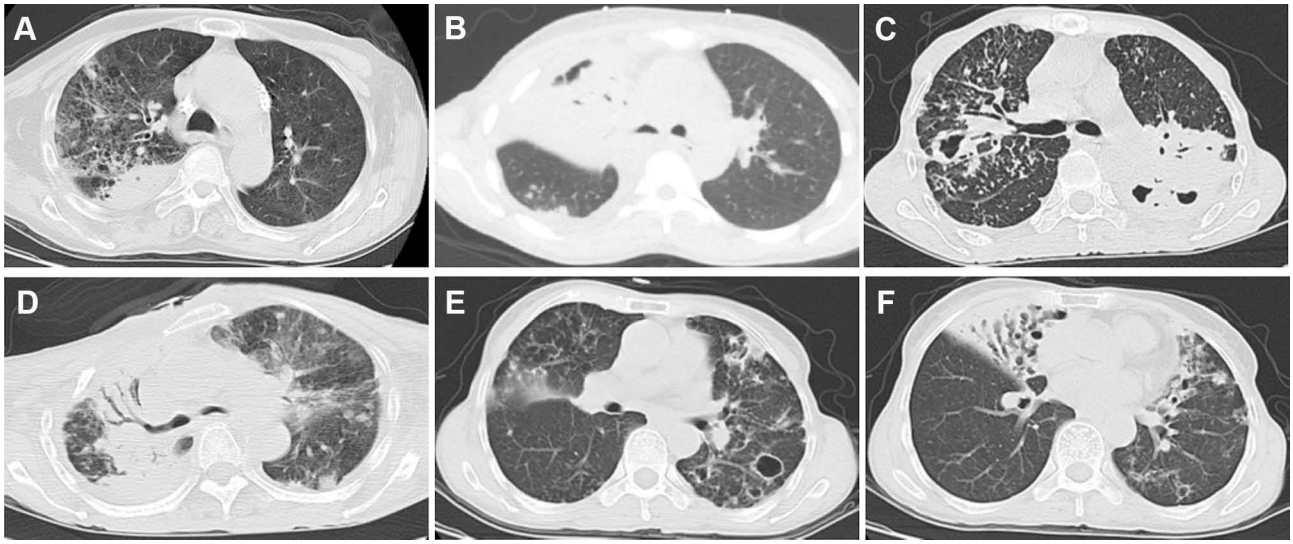

Figure 2 Chest computed tomography (CT) showing exudation and consolidation in the upper lobe of the right lung (**A** from patient 3); atelectasis in the middle lobe of the right lung and right pleural effusion (**B** from patient 7); consolidation in the lower lobe dorsal segment of the left lung with cavity formation and thick-walled cavities, nodules, patches, and fiber proliferation in the upper lobe of the right lung (**C** from patient 8); right thoracic collapse, large consolidation in the upper lobe of the right lung with air bronchogram signs, and multiple ground-glass opacities, patchy exudations and nodules in the upper lobe of the left lung (**D** from patient 1). Multiple patchy exudations, bronchiectasis and multiple thin-walled cavities of varied sizes in the lower lobe of the bilateral lung (**E** from patient 8). Multiple areas of bronchiectasis, consolidation and exudation in the middle lobe of the right and left lungs (**F** from patient 8).

treatment. Two patients died of comorbidities during the treatment period. Patient 1, who had chronic obstructive pulmonary disease (COPD) was misdiagnosed with tuberculosis for one and a half years and finally died of respiratory and circulatory failure and septic shock after 27 days of treatment for DNTM disease. Patient 6, who had diabetes, died of hypoglycemic coma after the diagnosis of DNTM disease and treatment for 2 years. The remaining patient was lost to follow-up (Table 3 and Supplemental Table 3).

Discussion

Nontuberculous mycobacteria are regarded as opportunistic pathogens and have been reported in immunosuppressed individuals.[12,13] In recent years, several studies demonstrated that AIGAs may be an important susceptibility factor for NTM infections in previously healthy individuals.[3,14] Hase et al[3] found that 34% AIGA-positive patients with NTM disease have bone and joint involvement by reviewing 111 AIGA-positive patients with NTM disease. In this study, all ten patients had multiple osteolytic destructions and 70% of these patients with positive AIGAs, which were confirmed in the previous research. These phenomenon suggests that NTM infection of bone is not rare in AIGA-positive patients, and the mechanism of osteolysis may be related to AIGAs.[4,5] NTM infection and inflammation break the balance of osteoclast formation and bone destruction, resulting in a bias toward bone resorption.[4] In addition, NTM infection of bone has been rarely reported and is often overlooked by clinicians.

[17] Interferon-γ (IFN-γ) is important in the maintenance of the balance between osteoclasts and osteoblasts. Osteoclast formation and bone destruction were more pronounced in mice lacking a functional IFN-γ.[15,16] IFN-γ directly inhibit osteoclast formation from osteoclast precursors, and indirectly stimulate osteoclast formation by stimulating antigen-dependent T-cell activation and secretion of the osteoclastogenic factors RANKL and TNF-α.[17] Recently, blockade effects of AIGAs present in NTM patients on IFN-γ have been described by several studies, suggesting that AIGAs can neutralize IFN-γ, affect the activation of the IFN-γ receptor (IFN-γR) and downregulate the production of its downstream factors (eg, TNF-α and IL-12), and inhibit IFN-γ-STAT-1 phosphorylation.[18] Thus, osteolytic lesions in NTM patients with positive AIGAs may be due to the blockade and neutralizing effects of AIGAs on anti-IFN-γ, leading to a disruption in the balance between osteoclasts and osteoblasts, NTM infection and inflammation bias toward bone resorption.

In our study, all patients presented with fever, emaciation, anemia, ostealgia, subcutaneous abscess and markedly increased leukocytes counts, CRP concentrations and ESRs. Chest CT revealed extensive and multiple

Table 2 Imaging Manifestations of 10 Patients with Disseminated *Nontuberculous mycobacteria* Disease with Osteolytic Lesions

Patient	Involvement of the Lung Lobes and Lung Segments	Findings on Chest Computed Tomography (CT)	Bone Imaging Features
P1	Upper middle lobe and lower lobe dorsal segment of the right lung; left lung	Cavities, patchy exudation, fibrous proliferation, ground-glass opacity, nodules, pleural thickening, pleural effusion, pericardial effusion and bronchiectasis	CT revealed irregular bony destruction in the sternum with surrounding abscess formation; X-ray imaging revealed destruction of the cortical substance of bone in the right second anterior rib with surrounding callus formation.
P2	None	No abnormal findings	CT revealed patchy and irregular destruction of the bone, bone defect in the mandible with surrounding abscess formation.
P3	Upper middle lobe and lower lobe dorsal segment of the right lung; left lung	Patchy exudation, fibrous proliferation, ground-glass opacity, consolidation, pleural thickening, pleural effusion, pericardial effusion, bronchiectasis, increase and calcification of the mediastinal and hilar lymph node	CT revealed multiple moth-eaten and irregular destruction of the bone, narrowing of the joint space and surrounding abscess formation in the right wrist joint, metacarpus and thumb; irregular bony destruction, bone defect, sequestrum formation, narrowing of the hip joint space and surrounding abscess formation in the left acetabulum, femoral head and ilium.
P4	Right lung; upper lobe and lower lobe dorsal segment of the left lung	Patchy exudation, fibrous proliferation, ground-glass opacity, pleural thickening, pleural effusion, pericardial effusion and bronchiectasis	CT revealed moth-eaten and patchy, irregular destruction of the bone, bone defect, narrowing of the intervertebral space, surrounding abscess formation and bone proliferation cirrhosis in the C7 vertebral body and the T1, T2 vertebral bodies.
P5	Upper middle lobe of the right lung; left lung	Patchy exudation, fibrous proliferation, consolidation, pleural thickening, pleural effusion and atelectasis	CT revealed patchy and irregular destruction of the bone in the inner plate of the left frontal bone with surrounding abscess formation; X-ray imaging revealed bone fracture in the right clavicle.
P6	Upper lobe of the right lung; upper lobe apicoposterior segment of the left lung; lower lobe dorsal segment, posterior basal segment of the bilateral lung	Patchy exudation, fibrous proliferation, consolidation, pleural thickening, and bronchiectasis	CT revealed moth-eaten and patchy, irregular destruction of the bone and multiple, well-circumscribed, rounded low-density areas with bone destruction in the sternum, the right first and second anterior ribs, right scapula and humerus with surrounding abscess formation; X-ray imaging revealed a bone fracture in the right clavicle.
P7	Right lung; upper lobe lower tongue segment and lower lobe of the left lung	Cavities, patchy exudation, fibrous proliferation, consolidation, nodules, mediastinal and hilar lymphadenopathy	X-ray imaging revealed a single, well-circumscribed, rounded low-density area with bone destruction in the tibia and talus.

(*Continued*)

Table 2 (Continued).

Patient	Involvement of the Lung Lobes and Lung Segments	Findings on Chest Computed Tomography (CT)	Bone Imaging Features
P8	Right lung; upper lobe tongue segment, lower lobe anterior inner basal segment and dorsal segment of the left lung	Cavities, Patchy exudation, fibrous proliferation, consolidation, nodules, pleural thickening, pleural effusion, bronchiectasis, mediastinal and hilar lymphadenopathy	CT revealed an irregular bone defect in the manubrium of the sternum with a sclerotic edge. MRI scan revealed high signals in the T10 vertebral body, the L3 vertebral body, sacrum, ilium and femoral head in the T2-weighted image and the fat-saturated T2-weighted image. ECT revealed increased radioactive concentration in the manubrium of the sternum, multiple ribs, the L3 vertebral body, bilateral sacroiliac joints, upper end of the right femur, left ilium and left knee joint. PET/CT showed metabolic activity in multiple bones of the body.
P9	Lower lobe dorsal segment of the bilateral lung	Patchy exudation, hilar lymphadenopathy and atelectasis	PET/CT showed whole-body bone metabolic activity.
P10	None	No abnormal findings	CT revealed moth-eaten destruction of bone in the left clavicle, the C7 vertebral body and the L1 vertebral body with surrounding abscess formation.

pulmonary parenchymal exudations, consolidation, cavities, and bronchiectasis, while radiography and bone CT revealed osteolytic lesions. Histopathological examination revealed suppurative granulomas in the lesions. These clinical and laboratory findings, variable imaging manifestations, and histopathological changes resemble those seen in osteomyelitis caused by tuberculosis. Thus, all patients were misdiagnosed with tuberculosis before being diagnosed with NTM infection. These results indicate insufficient recognition of DNTM disease with osteolysis by clinicians. Therefore, systemic research on NTM infection of bone that investigates clinical characteristics, especially radiographic presentations, should be considered a necessity for improving differential diagnosis.

According to our research, the clinical characteristics of disseminated NTM infection of bone leading to osteolytic lesions can be summarized as follows: (1) NTM infection is mainly characterized by chronic suppurative infection manifesting as significantly increased white blood cell and neutrophil counts, ESR concentrations and CRP levels, and wasting systemic symptoms such as anemia and hypoproteinemia may be obvious. In addition, NTM infection commonly presents as disseminated infection of multiple organs including the lungs, lymph nodes, skin, bone and joints, with multiple subcutaneous abscesses, increased purulent secretions in the airway and suppurative changes in lymph nodes with pain. (2) NTM can affect any bone of the body, often presenting as multiple bone involvement. The most commonly involved sites were the vertebrae, sternum, clavicle and ribs, followed by the femur and ilium. The humerus, scapula, metacarpal, phalanx, tibia, talus, frontal bone and mandible were also involved. Radiography and CT of bone revealed osteolytic lesions characterized by multiple lucent defects showing moth-eaten or irregular destruction of bone, bone defects, well-circumscribed, rounded low-density areas, pathological fractures, and periosteal proliferation. Bone ECT showed significantly increased uptake in multiple bones, while PET/CT showed metabolic activity in multiple bones of the body. When NTM disseminates to an osseous site, significant focal neutrophil aggregation and lysosome release leads to ostealgia, subcutaneous abscess and osteolytic destruction. (3) Histopathological examination of pathological tissue specimens obtained from patients with

Table 3 Treatment and Outcomes of 10 Patients with Disseminated Nontuberculous Mycobacterial Disease with Osteolytic Lesions

Patient	Anti-NTM Therapy	Therapy for Coinfections	Treatment Duration	Surgical Treatment	Retreatment	Outcome
P1	MXF+CLR+EMB+RFB	ITC for antifungal	27 days	Debridement of lesions on the right chest wall	None	Died
P2	INH+RFP+EMB+CLR	None	18 months	Incision and drainage of a left maxillofacial abscess	None	Cured
P3	INH+RFP+LVFX+PTO	None	29 months	Debridement of lesions on the left ilium, right wrist joint and left hip joint	None	Cured
P4	EMB+LVFX+RFT+DIP for 18 mon; DIP+RFT+EMB+VM for 14 mon; LVFX+RFP+EMB +CLR for 15 mon; AMK +MXF+EMB+CLR for 18 mon	FLC for antifungal	65 months	None	7 times	Cured
P5	PTO+PZA+CLR+SXT	FLC, AMB and ITC for antifungal; CXM, SCF and PTZ for antibiotic	24 months	Debridement of lesions on the right chest wall; open reduction and internal fixation for fracture of the right clavicle	None	Cured
P6	LVFX+SXT for 18 mon; CLR+SXT+EMB for 3 mon	PEN and AMK for antibiotic	21 months	None	4 times	Died
P7	PTO+MXF+CLR+RFB	None	30 months	None	1 time	Cured
P8	EMB+CLR+RFB	AMB and ITC for antifungal	18 months	None	None	Cured
P9	INH+RFP+SXT+EMB	VCZ for antifungal; PTZ and LVFX for antibiotic	Unknown	Unknown	Unknown	Lost
P10	LVFX+SXT+CLR	None	18 months	Debridement and drainage of lesions on the lumbar spine and left clavicle; internal fixation of the lumbar spine	None	Cured

Abbreviations: AMK, amikacin; AMB, amphotericin B liposome; CLR, clarithromycin; CXM, cefuroxime; DIP, dipasic; EMB, ethambutol; FLC, fluconazole; INH, isoniazid; ITC, itraconazole; LVFX, levofloxacin; MXF, moxifloxacin; PZA, pyrazinamide; PTZ, piperacillin-tazobactam; PTO, protionamide; PEN, penicillin; RPF, rifampicin; RFB, rifabutin; RFT, rifapentine; SXT, compound sulfamethoxazole; SCF, sulbactam and cefoperazone; VM, viomycin; VCZ, voriconazole.

NTM infection demonstrated suppurative inflammation dominated by neutrophil infiltration, with or without granuloma formation. Compared with osteoarticular infections caused by NTM, infections caused by tuberculosis most commonly involve the thoracolumbar region of the spine and load-bearing joints such as the hips and knees.[19] Imaging examinations revealed sequestrum in the bony destruction area, intervertebral disc destruction, paravertebral cold abscess and spinal deformity when tuberculosis bacteria infected bone.[6] Histopathology of pathological tissue specimens obtained from patients with tuberculosis demonstrates granulomas dominated by lymphocyte infiltration, with a central area of caseating necrosis.[6] Therefore, taking the typical clinical and imaging features and histopathological manifestations into consideration, osteolytic destruction caused by NTM

infection can be differentiated from that caused by tuberculosis, especially when the effect of anti-tuberculosis therapy is poor. Thus, etiological culture remains the gold standard for the diagnosis of NTM infection, tuberculosis and other fungal infections. In recent years, the development of molecular biology techniques, such as follow-up PCR, NGS and gene sequencing, has provided great help in the identification of mycobacterium strains and drug resistance profiles, greatly improving the clinical diagnosis rate and prognosis.[20–22]

According to guidelines,[9] for the treatment of DNTM disease, long-term chemotherapy with a combination of 5–6 antimycobacterial agents should be administered after species identification and in vitro AST for at least one to two years. For the treatment of DNTM disease with osteolytic lesions, systemic antimycobacterial chemotherapy should be primarily administered, though surgery can also play an important role in some cases. Surgical treatments, such as debridement and incision for drainage, should be considered in cases with poor response to chemotherapy, extensive bone destruction and abscesses formation.[9,23] For patients with pathological fractures, internal fixation of the fracture should also be performed immediately. In addition, long-term follow-up of DNTM patients with osteolysis after discharge is crucial to patient rehabilitation. The course and dosage of oral antibiotics, imaging examination findings, the ESR, and CRP levels should be monitored to assess the progression of the disease.[23] In addition, It has been reported that in the cases of bone and joint NTM infections, the most common causative NTM species are SGM dominated by the *M. avium-intracellulare complex*, while RGMs such as *M. fortuitum, M. abscessus* and *M. chelonae* have also been reported.[2,23] A multicenter retrospective study consisting of 117 patients with extrapulmonary NTM infections suggests that bone and joint infections were predictors of SGM infections.[24] These findings may be helpful in early empirical antimicrobial regimen selection for bone NTM infection in basic hospitals that are unable to identify subspecies.

Limitations

There were some limitations of our study. First, although this was a retrospective study, the number of patients included was not large. Furthermore, NTM patients without bone involvement were not included as a control group to calculate the incidence of NTM involving bone. Second, as a retrospective study, the medical record data of some of the patients were incomplete. Third, elucidating the reason why AIGA-positive patients with NTM infection are more prone to osteolytic destruction will require large, multicenter research, which will be done in subsequent studies. In spite of these limitations, we systematically analyzed the clinical and imaging characteristics of patients with NTM infection involving bone leading to osteolytic lesions for the first time, which provides information about this condition to clinicians and lays the foundation for further research.

Conclusions

DNTM infection of bone leading to osteolysis usually occurs in patients with AIGA-positive antibodies and is often misdiagnosed as tuberculosis. When patients present with increased white blood cell and neutrophil counts, focal suppurative granulomas, multiple areas with worm-eaten appearance or irregular destruction of bone with increased radioactive concentrations, DNTM disease with osteolytic lesions should be suspected, especially when the effect of antituberculous therapy is poor. On the basis of species identification and in vitro antimicrobial susceptibility testing, early systemic anti-nontuberculous chemotherapy, combined with surgical treatment if necessary, can improve the clinical efficacy and reduce the recurrence, disability and mortality of patients with DNTM disease with osteolytic lesions.

Data Sharing Statement

The datasets used or analyzed during the current study are available from the corresponding author on reasonable request.

Ethics Approval and Informed Consent

This study was approved by the Ethical Review Committee of the First Affiliated Hospital of Guangxi Medical University (2021. KY-E-118). Written informed consent was obtained from the patients for publication of this article and any accompanying images. Copies of the written consent forms are available for review. This study was conducted in accordance with the Declaration of Helsinki.

Acknowledgments

The authors thank Yanmei Shen, Professor of Imaging Medicine and Nuclear Medicine, Department of Imaging Medicine and Nuclear Medicine, the First Affiliated Hospital of Guangxi Medical University, and Zhili Li, Professor of Imaging Medicine and Nuclear Medicine, Department of Imaging Medicine and Nuclear Medicine,

Nanning Fourth People's Hospital. Mengxin Tang and Jie Huang are co-first authors for this study. Ye Qiu and Jianquan Zhang are co-correspondence authors for this study.

Author Contributions

M. Tang and J. Huang designed the study and analyzed the data. M. Tang wrote the draft of the manuscript. W. Zeng, Y. Huang and Y. Lei contributed to data collection. J. Zhang was responsible for critical revision of the manuscript. Y. Qiu helped perform the analysis and was involved in critical discussions. All authors contributed to data analysis and drafting or revising the article. All authors gave final approval of the version to be published, agreed to submission to the journal, and agree to be accountable for all aspects of the work.

Funding

This work was supported by grants from the Natural Science Foundation of China [NSFC81760010 and 82060364] and the Science and Technology Department of Guangxi Zhuang Autonomous Foundation of Guangxi Key Research and Development Program (No. GuikeAB20238025).

Disclosure

The authors report no conflicts of interest in this work.

References

1. Koh WJ. Nontuberculous mycobacteria-overview. *Microbiol Spectr*. 2017;5(1). doi:10.1128/microbiolspec.TNMI7-0024-2016
2. Kim CJ, Kim UJ, Kim HB, et al. Vertebral osteomyelitis caused by non-tuberculous mycobacteria: predisposing conditions and clinical characteristics of six cases and a review of 63 cases in the literature. *Infect Dis*. 2016;48(7):509–516. doi:10.3109/23744235.2016.1158418
3. Hase I, Morimoto K, Sakagami T, Ishii Y, van Ingen J. Patient ethnicity and causative species determine the manifestations of anti-interferon-gamma autoantibody-associated nontuberculous mycobacterial disease: a review. *Diagn Microbiol Infect Dis*. 2017;88(4):308–315. doi:10.1016/j.diagmicrobio.2017.05.011
4. Qiu Y, Zhang J, Li B, Shu H. Bacillus cereus isolated from a positive bone tissue culture in a patient with osteolysis and high-titer anti-interferon-γ autoantibodies: a case report. *Medicine*. 2019;98(43): e17609. doi:10.1097/MD.0000000000017609
5. Xu X, Lao X, Zhang C, et al. Chronic Mycobacterium avium skin and soft tissue infection complicated with scalp osteomyelitis possibly secondary to anti-interferon-γ autoantibody formation. *BMC Infect Dis*. 2019;19(1):203. doi:10.1186/s12879-019-3771-3
6. Leonard MK, Blumberg HM. Musculoskeletal tuberculosis. *Microbiol Spectr*. 2017;5:2. doi:10.1128/microbiolspec.TNMI7-0046-2017
7. Qiu Y, Zhang J, Liu G, et al. Retrospective analysis of 14 cases of disseminated Penicillium marneffei infection with osteolytic lesions. *BMC Infect Dis*. 2015;15:47. doi:10.1186/s12879-015-0782-6
8. Molter CM, Zuba JR, Papendick R. Cryptococcus gattii osteomyelitis and compounded itraconazole treatment failure in a Pesquet's parrot (Psittrichas fulgidus). *J Zoo Wildl Med*. 2014;45(1):127–133. doi:10.1638/2013-0042R1.1
9. Griffith DE, Aksamit T, Brown-Elliott BA, et al. An official ATS/IDSA statement: diagnosis, treatment, and prevention of nontuberculous mycobacterial diseases. *Am J Respir Crit Care Med*. 2007;175 (4):367–416. doi:10.1164/rccm.200604-571ST
10. Haworth CS, Banks J, Capstick T, et al. British Thoracic Society guidelines for the management of non-tuberculous mycobacterial pulmonary disease (NTM-PD). *Thorax*. 2017;72(Suppl2):ii1–ii64.
11. Daley CL, Iaccarino JM, Lange C, et al. Treatment of nontuberculous mycobacterial pulmonary disease: an official ATS/ERS/ESCMID/IDSA clinical practice guideline. *Eur Respir J*. 2020;56(1):2000535. doi:10.1183/13993003.00535-2020
12. Nunes-Costa D, Alarico S, Dalcolmo MP, Correia-Neves M, Empadinhas N. The looming tide of nontuberculous mycobacterial infections in Portugal and Brazil. *Tuberculosis*. 2016;96:107–119. doi:10.1016/j.tube.2015.09.006
13. Henkle E, Winthrop KL, Le T, Kinh NV, Cuc NTK. Nontuberculous mycobacteria infections in immunosuppressed hosts. *Clin Chest Med*. 2015;36(1):91–99. doi:10.1016/j.ccm.2014.11.002
14. Browne SK. Anticytokine autoantibody-associated immunodeficiency. *Annu Rev Immunol*. 2014;32:635–657. doi:10.1146/annurev-immunol-032713-120222
15. Takayanagi H, Ogasawara K, Hida S, et al. T-cell-mediated regulation of osteoclastogenesis by signalling cross-talk between RANKL and IFN-gamma. *Nature*. 2000;408(6812):600–605. doi:10.1038/35046102
16. Kelchtermans H, Billiau A, Matthys P. How interferon-gamma keeps autoimmune diseases in check. *Trends Immunol*. 2008;29 (10):479–486. doi:10.1016/j.it.2008.07.002
17. Gao Y, Grassi F, Ryan MR, et al. IFN-gamma stimulates osteoclast formation and bone loss in vivo via antigen-driven T cell activation. *J Clin Invest*. 2007;117(1):122–132. doi:10.1172/JCI30074
18. Krisnawati DI, Liu Y-C, Lee Y-J, et al. Blockade effects of anti-interferon- (IFN-) gamma autoantibodies on IFN-gamma-regulated antimicrobial immunity. *J Immunol Res*. 2019;2019:16 29258. doi:10.1155/2019/1629258
19. Hogan JI, Hurtado RM, Nelson SB. Mycobacterial musculoskeletal infections. *Infect Dis Clin North Am*. 2017;31(2):369–382. doi:10.1016/j.idc.2017.01.007
20. Zhou X, Wu H, Ruan Q, et al. Clinical evaluation of diagnosis efficacy of active mycobacterium tuberculosis complex infection via metagenomic next-generation sequencing of direct clinical samples. *Front Cell Infect Microbiol*. 2019;9:351. doi:10.3389/fcimb.2019.00351
21. Huang Z, Zhang C, Fang X, et al. Identification of musculoskeletal infection with non-tuberculous mycobacterium using metagenomic sequencing. *J Infect*. 2019;78(2):158–169. doi:10.1016/j.jinf.2018.10.002
22. Rahman MM, Rahim MR, Khaled A, Nasir TA, Nasrin F, Hasan MA. Molecular detection and differentiation of mycobacterium tuberculosis complex and non-tuberculous mycobacterium in the clinical specimens by real time PCR. *Mymensingh Med J*. 2017;26(3):614–620.
23. Bi S, Hu FS, Yu HY, et al. Nontuberculous mycobacterial osteomyelitis. *Infect Dis*. 2015;47(10):673–685. doi:10.3109/23744235.2015.1040445
24. Kim JH, Jung IY, Song JE, et al. Profiles of extrapulmonary non-tuberculous mycobacteria infections and predictors for species: a multicenter retrospective study. *Pathogens*. 2020;9(11):949. doi:10.3390/pathogens9110949